International Journal of Scientific Engineering and Technology (ISSN : 2277-1581)
Volume No2, Issue No.9, pp : 817-821 1 Sept 2013

Synthesis and Characterization of Fe-Catalyst for Fischer-Tropsch Synthesis Using Biosyngas

Hanif A. Choudhury, Vijayanand S. Moholkar
[1]Center for Energy, [2]Centre for Energy and Department of CE, IIT Guwahati,
Guwahati-781039, Assam, India
E-mail: vmoholkar@iitg.ac.in; c.hanif@iitg.ernet.in

Abstract*—Fischer–Tropsch technology has gathered renewed interest in the energy industry in recent times for synthesis of diesel and gasoline. The synthesis of linear hydrocarbon diesel fuel (having high cetane number) through Fischer–Tropsch synthesis (FTS) reaction requires syngas with high H_2/CO molar ratio. Producer gas obtained from biomass gasification has low H_2/CO ratios, with significant content of CO_2, and hence, is not suitable as feed for FT synthesis using conventional transition metal (usually cobalt and nickel) based catalysts. Catalysts having high water gas shift reaction (WGS) activity are suitable for FT synthesis with biomass derived producer gas, as WGS reaction can compensate for H_2 deficiency. Iron catalysts are well-known for their FTS as well as WGS activity. In this study, co-precipitated Fe-catalysts with different metal promoters have been synthesized and characterized In this work, we have attempted to identify different intermediate phases involved during transformation of the catalyst. We have done the catalyst characterization using several techniques such as XRD, BET & TPR techniques.

Key words: Promoted Iron catalyst, Biosyngas, Coprecipitaion, Iron carbide

I. Introduction

Fischer–Tropsch synthesis (FTS) has been a well-known process for production of liquid hydrocarbons or liquid fuels from synthesis gas (or syn gas as it is popularly known) [1-5]. Syngas is a mixture of carbon monoxide (CO) and hydrogen (H_2), typically in the 1:2 molar ratio. Syngas can be derived from gasification of coal, biomass or steam reforming of natural gas. Conventional feed stock for FTS is natural gas, however, steam reforming of methane being an endothermic process, its energy requirements are excessively high that adversely affects the process economy [6]. From point of view of basic chemical mechanism, the FTS is a surface polymerization reaction, where a transition metal catalyst is necessary to bring out synthesis of liquid fuels. Producer gas from biomass gasification (with typical composition of 15% H_2, 20% CO, 20% CO_2, 5% CH_4 and balance N_2) can form alternate feedstock to syngas for FTS reaction. However, utilization of biomass derived produced gas (which is also termed by biosyngas by some authors) has its own limitations for FTS reaction. Major problem with biosyngas is its sub-stoichiometric composition, in that the H_2/CO molar ratio is always approximately ≤ 1, whereas typical molar ratio requirement of H_2/CO for FTS reaction is ~ 2. Therefore, FTS reaction with conventional transition metal catalyst cannot use the biosyngas. The deficiency of H_2 in the biosyngas can be met through water gas shift reaction (WGS). Catalyst plays an important role in the FTS reaction, and hence, choice of catalyst is a critical component of the success of the process. When it comes to FTS synthesis from biosyngas, iron oxides have been used very extensively [7]. Iron oxides are active in both water gas shift (WGS) and reverse water gas shift reactions (RWGS) [7], and they are considered as the ideal catalysts for the FTS of CO_2-containing syngas feeds [8]. However, when used in pure form (without any promoters), Fe-based catalysts offer high selectivity to non-desired products such as methane. They also undergo rapid deactivation. In order to make the iron catalyst active, selective and stable, several promoters and stabilizers are used. The active phase of the catalyst is believed to be the iron carbide species, while the contribution by iron oxide/ metallic iron is also being investigated. It is very difficult to pin point the nature of active phase as the iron based catalysts change their phases during the reaction from the Fe_2O_3 to Fe_3O_4, and further to metallic Fe to iron carbides [9]. The final active site depends upon the nature of the precursor used, its pre-treatment and the operating conditions. It is well known that the promotion by potassium has significant effect on the FTS performance of catalysts. Potassium promotes the chain-growth of hydrocarbons (thus suppressing production of methane) and also improves the selectivity of hydrocarbon product from FT process. The correlation studies between catalysts surface basicity and hydrocarbon selectivity reveals that the surface basicity can apparently suppress the methane selectivity. Other promoters such as Zn have no influence on the redox properties of the active metal (i.e., Fe), however it increases the H_2 adsorption on ZnO surface that facilitates the WGS reaction [10]. Further, promoters like Cu facilitate the reduction of Fe^{3+} to Fe^{2+}. Presence of ZnO facilitates the reduction of CuO to Cu [5]. Al_2O_3 was selected as structural promoter for the catalyst,

since it increases the dispersion of K on the Fe-Alumina catalyst. In the present study, a co-precipitated Fe-catalyst with various metal promoters for possible use in FTS reaction has been synthesized. The main objective of this work is to enhance the reduction behavior and also to make it easily transformable to active carbide phases of FTS reaction.

II. Experimental

Catalysts preparation

Aqueous solutions of $Fe(NO_3)_3$ $9H_2O$(0.5M) (Merk, India) and $Cu(NO_3)_3 3H_2O$(0.5M), $Al(NO_3)_3 9H_2O$ (0.5M), $Zn(NO_3)_3$ with appropriate molar ratio were premixed and the resulting solution was added drop wise to heated(70 ^oC) aqueous solution of Na_2CO_3 (0.5M) (Merk, India) in a two neck round bottom flask. The mixed nitrate solution was continuously stirred with a hot plate magnetic stirrer at 600 rpm whilst the temperature was maintained isothermally at 70 ^oC by means of a thermostat. The pH of the solution maintained at 7 by means of (0.05MHCl) and (0.1 M NH_4OH). The procedure took approximately 10 minutes to complete. The resulting precipitate was then left in the medium at the same temperature and for 24 h. The precipitate was first filtered and washed with deionized water for several times to remove any Cl^- /Na. Chloride removal was confirmed by $AgNO_3$ test while sodium removal was confirmed by atomic absorption spectroscopy (AAS). The precipitate then dried at 110 ^oC in the oven for 16 h to give the material denoted as the catalyst precursor which was subsequently calcined in static air in the muffle furnace (650 ^oC, 5 h). The catalyst was then promoted with K by adding (5 wt % of KNO_3 (Loba Chemical, India) by wetness impregnation at a pH of 7.5. Finally the catalyst with composition of 65Fe/10Cu/10Zn/10Al/5K was synthesized and named as Fe/Cu/Zn/Al/K. Similarly the catalyst with composition90Fe/10 Al is also synthesized and named as Fe/Al.

Catalyst Characterization

X-Ray Diffraction (XRD)

Powder X-ray diffraction (XRD) measurements were performed using a Bruker Axs Company, D8 Advance diffractometer (Germany). Scans were taken with a 2θ stepsize of 0.02 and a counting time of 1 second using CuKα radiation source generated at 40 kV and 30 mA. Data was collected over a 2θ range from 10^o to 70^o and phases were identified by matching experimental patterns to entries in the JCPDF2.

BET Measurements

Brunauer-Emmett-Teller surface area BET surface areas, pore volumes and average pore diameters were determined by N_2 physisorption at 77 K using a Beckman Coulter, Model: A53878. A 0.3 g catalyst sample was degassed at 300 ^oC for 2 h and then heated at 10 ^oC/min to 300 ^oC and held for 2 h before analysis.

Temperature-programmed reduction (TPR)

H_2-TPR was performed using Micromeritics TPD/TPR 2720 system to determine reducibility of the calcined iron catalysts. For H_2-TPR the catalysts (0.50 g) were reduced in a flow of 5% H_2/Ar (30 cc/min) with a ramp rate of 10 ^oC/min to 800 ^oC. A thermal conductivity detector (TCD) was used to measure H_2 consumption. The detector output was calibrated based upon 100% reducibility of Ag_2O powder, and a H_2O trap was used to remove H_2O produced during the reduction. The degree of reduction of the catalyst was calculated as follows by using data from TPR.

$$(\%)\ \text{reduction} = \frac{[H_2\ \text{consumption below } 450^oC]}{\text{Total } H_2\ \text{consumption in TPR experiment}} \times 100$$

Eq(1)

III. Results and Discussion

Iron catalysts show a complex behavior, and their actual composition during FTS reaction remains a paradox. During FTS reaction, one phase of iron transforms to another, and then the FTS reaction begins. Several authors have reported that the carbide phase of iron is active for FTS reaction. Further promotion of iron catalyst with appropriate metal promoters would bring stability of catalyst, making it easily reducible and selective towards the desired long chain hydrocarbons. In view of the above, we synthesized two catalysts, viz. one with different metal promoters, and the other with pure iron with Al as structural promoter. We have discussed the reduction behavior of both catalysts in the next section with H_2–TPR study. H_2–TPR study is an important yardstick for assessing potential of a FTS catalyst, since every metal oxide is not FTS active. Therefore, the catalyst has to be transformed to its active phase. The transformation of iron catalyst under H_2 gas follows the following trend; $Fe_2O_3 \rightarrow Fe_3O_4 \rightarrow \alpha$–Fe. But metallic α–Fe is not also FTS active. During FTS reaction, the iron catalyst is reduced with constant flow of H_2 or CO gas as pre–treatment step for a considerable amount of time. After the initial pretreatment step, the syngas is admitted for the FTS reaction. Initially, CO and H_2 have dissociative adsorption on the surface of the metallic iron particle. At the reaction temperature (300 ^oC), the metallic iron is converted to iron carbide and some of the catalyst is also lost because of oxidation due to the formation of water reacting with surface bound H_2. We have not carried out any FTS reaction with the synthesized catalyst, but rather have

reduced the catalyst under flow of 5% H_2/Ar gas (30 cc/min) with a ramp rate of 10 ^oC/min to 800 ^oC. The reduced catalysts were then subjected to the flow of 30% CO/N_2 gas (30 cc/min) for 1 h at 300 ^oC at atmospheric pressure. Subsequently, the catalyst was characterized by XRD to observe the phase change.

H_2–TPR

Fig. 1 shows the reduction profiles of two catalysts under the flow of H_2 gas. The TPR profile of both catalysts shows reduction profiles with (an expected) 2–step reduction process of α–Fe_2O_3 to α–Fe. The first step in ascribed to the reduction of $Fe_2O_3 \rightarrow Fe_3O_4$. The reduction $CuO \rightarrow Cu$ also falls in the same range, and hence, an overlap peak for the promoted catalyst was observed. CuO present in the promoted samples contributes to the consumption of H_2. However, because of the strong influence of CuO morphology on the observed T_{max} values in TPR experiments, and the overlap of Fe and Cu reduction peaks, it was not possible to reliably estimate the contribution of the CuO species to H_2 uptake from of the TPR peaks. However, a clear shift in the onset of the first reduction step is observed in the Cu–promoted catalyst. While the unpromoted catalyst shows two peaks (T_{max} = 438 ^oC and 524^oC), the promoted catalysts show two major contribution, with T_{max} at 252 ^oC and 291^oC. The peaks are ascribed to the two step reduction of Fe^{3+} in α–Fe_2O_3 to Fe^{2+} in the mixed $Fe^{2+/3+}$ inverse spinel Fe_3O_4 structure. The presence of peak around 650–700^oC is an indication of difficulty in reduction of FeO to α–Fe for which high temperature is required. The Fe/Cu/Zn/Al/K catalyst shows a suppressed amount of H_2 uptake at higher temperatures, indicative for a limited extent of reduction beyond Fe^{2+}. As an indication of the total extent of reduction of the catalysts, Fig. 1 also shows the total cumulative amount of H_2 uptake during the TPR experiment. These results clearly illustrate the influence of Cu on the bulk reduction properties of the catalysts. Both reduction steps, viz. from Fe^{3+} to Fe^{2+}, and Fe^{2+} to FeO, are facilitated in the presence of Cu. Presence of Zn in the catalyst facilitates the reduction of Cu, which in turn facilitates the reduction of Fe by increasing the spill over of H_2 . Al does not directly play any role in the reduction process, but provides attrition resistance to the catalyst, which prevents its sintering at higher reaction temperature. Excessive presence of Al may result in formation Fe-alumina species that reduces the active metal content in the catalyst. A possible solution for this problem is optimization of the amount of Al in the catalyst (not attempted in this work).

BET analysis.

The BET surface area with percent reduction (under H_2 gas) of the promoted and un-promoted catalyst is given in Table 1. The BET surface area of the Fe/Cu/Zn/Al /K is ~ 50 m^2/g, whereas the BET surface area of the Fe/Al samples is 20.56 m^2/g. There is a sharp increase in the surface area with presence of promoters, which can be visible from the adsorption isotherms presented in Fig. 2. The increase in the surface area is attributed to the higher dispersion of CuO and ZnO on the Fe_2O_3. Fig. 3 presents the pore volume distribution of both the catalyst with their pore diameter. For both catalysts, the median of pore size distribution is ~ 30 nm. An interesting result is observed from the pore volume data that the unpromoted catalyst have very small pore volume as compared to the promoted one. In fact, the unpromoted catalyst has almost non-porous character, which is evident from the smaller BET surface area.

Table 1: Promoted and unpromoted catalyst surface properties

Catalyst	BET Surface area(m^2/g)	% Reduction[a]
Fe/Al	20.56	3
Fe/Cu/Zn/Al/K	~ 50	21

a= calculatied by using equation (1)

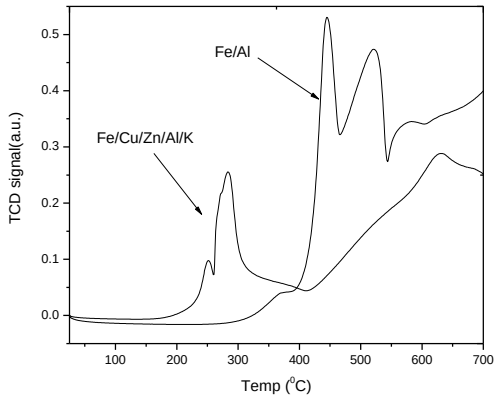

Figure 1:H_2-TPR of the catalysts. (a) Fe catalyst on Al-support, (b) Iron catalyst promoted with K, Cu and Zn

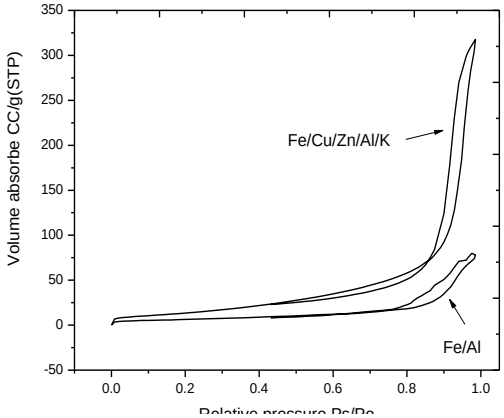

Figure.2: N_2 Adsorption-desorption isotherm for Fe/Cu/Zn/Al/K and Fe/Al catalyst

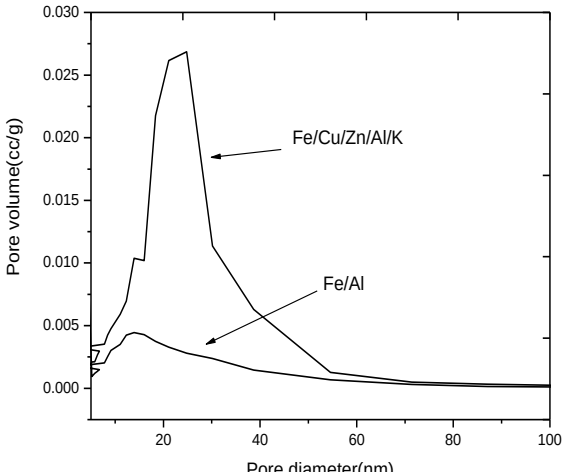

Figure 3: Pore diameter distribution with pore volume for Fe/Cu/Zn/Al/K and Fe/Al catalyst

XRD analysis

Fig. 4 shows the XRD patterns of all the catalyst obtained with different reactions protocol. The XRD spectrum marked as (a) is for the promoted catalyst (Fe/Cu/Zn/Al/K) after the calcination. The XRD spectrum marked as (b) is for the same catalyst after the CO treatment, while the XRD spectrum marked as (c) is the unpromoted catalyst (Fe/Al) after CO treatment.

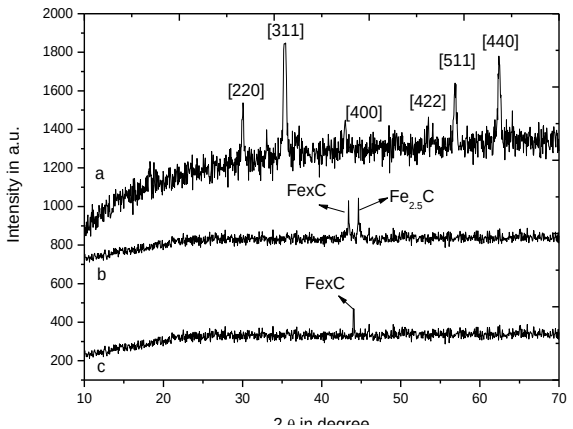

Figure 4: XRD diffraction pattern of the calcined catalysts (a) Fe/Cu/Zn/Al/K before CO treatment (b) Fe/Cu/Zn/Al/K after CO treatment (c) Fe/ Al after CO treatment

The pattern of the promoted calcined catalyst matches well with the standard patterns of $Cu_{0.5}Zn_{0.5}Fe_2O_4$ (JCPDS file no. 770012). All the peak pattern of the solid samples can be readily indexed to $Cu_{0.5}Zn_{0.5}Fe_2O_4$, where the diffraction peaks at 2θ values of 30.1, 35.46, 43.10, 53.47, 57.00, and 62.59° can be ascribed to the reflection of (220), (311), (400), (422), (511), and (440) planes of the $Cu_{0.5}Zn_{0.5}Fe_2O_4$, respectively. Very low intensity peaks at 2θ diffraction values of 15.45, 16.22 and 19.59 corresponds to Al_2O_3 (JCPDF file no. 861410). However, there are a number of unidentified weak intensity peaks present in between the 2θ range of 30 to 65° also corresponds to the Al_2O_3 and K_2O (JCPDF file no. 772176). The highly intense peak from the $Cu_{0.5}Zn_{0.5}Fe_2O_4$ overlaps in this region, and hence, precise indexing of Al_2O_3 and K_2O were not possible for this study. Spectrum (b) shows growth of two peaks near 42–44°, whereas the XRD spectrum (c) shows a growth of new peak at 43.4°. These peaks have been indexed with χ–CFe2.5 (JCPDF2 file no 361248). From the XRD spectra of the catalyst before and after CO treatment, it is clearly visible that the catalysts are transformed to the corresponding carbide phases, which are essential for the FTS reaction. It was also noted that Fe_2O_3 reacted with Cu and Zn during calcination and formed a mixed metal oxide $Cu_{0.5}Zn_{0.5}Fe_2O_4$. These types of composition of metals are very good catalyst for water gas shift reaction activity reported previously.

IV. Conclusion

Metal promoters have marked effect on the reduction properties of co–precipitated iron catalyst. The TPR profile of the promoted and unpromoted catalyst illustrates different extent of reduction. The promoted catalyst has a high degree of reduction (21%) because of the metal promoters. The presence of Zn facilitates the reduction [10] of Cu, and which intern facilitates the reduction of the Fe^{3+} to α–Fe. Major shortcoming of the co–precipitated iron catalyst, as revealed in this study, is the agglomeration of the iron particles because of the paramagnetic nature of the Fe^{3+}. The powder XRD pattern of the catalyst before and after the CO treatment reveals the phase transformation from the magnetite to iron carbide phases. The χ–$Fe_{2.5}C$ is believed to be the active phase for FTS reaction [13] and the synthesized catalyst has transformed to corresponding carbides after CO treatment. It is observed that the promoted and unpromoted catalyst transformed to the carbide phases, but the promoted one has more carbide phase than the unpromoted one. Moreover, the unpromoted catalyst was not very porous as compared to the promoted catalyst. The porosity of catalyst material is an important characteristic as it increases the surface area for the reaction. On a whole, the characteristics of the catalyst synthesized in this study endorse its suitability for FTS reaction utilizing biosyngas. However, controlling particle size, avoiding agglomeration and increase surface properties may greatly enhance the catalytic property of the catalyst, which remains as a challenge for future studies.

Acknowledgements

The author wishes to acknowledge Ministry of New and Renewable Energy (MNRE), Government of India for funding (vide ref.19/20/2007–R&D/BE) of the project. Mr. Hanif A. Choudhury also acknowledges MNRE for financial support during this research work through National Renewable Energy Fellowship. The SEM facility provided by CIF, IIT Guwahati is gratefully acknowledged.

References

i. A N Pour, S M K Shahri, Y Zamani, A Zamanian, "Promoter effect on the CO_2–H_2O formation during Fischer–Tropsch synthesis on iron–based catalysts," Journal of. Natral Gas Chemistry, vol. 19, no. 2, pp. 193–197, (2010).

ii. E. de Smit, F. M. F. de Groot, R. Blume, M. Havecker, A. Knop–Gericke, B. M. Weckhuysen, "The role of Cu on the reduction behavior and surface properties of Fe–based Fischer–Tropsch catalyst," Physical Chemistry Chemical Physics, vol. 12, no. 3, pp. 667–680 (2010).

iii. J. W. Cheon, S. H. Kang, J. W. Bae, S. J. Park, K. W. Jun, G. M. Dhar, K. L. Lee, "Effect of active component contents to catalytic performance on Fe–Cu–K/ZSM5 Fischer–Tropsch catalyst," Catalysis Letters, vol. 34, no. 1-2, pp. 233–241, (2010).

iv. M. Dinga, Y. Yang, B. Wu, J. Xu, C. Zhang, H. Xianga, Y. Li, "Study of phase transformation and catalytic performance on precipitated iron–based catalyst for Fischer–Tropsch synthesis, " Journal of Molecular. Catalysis A: Chemical, vol. 303, no. 1-2, pp. 65–71, (2009).

v. A. Sarkar, R. A. Keogh, S. Bao, B. H. Davis, "Fischer–Tropsch synthesis with promoted iron catalyst: Reaction pathways for acetic acid, glycol, 2 ethoxyethanol and 1,2–diethoxyethane, " Applied Catalysis A:General, vol. 341, no. 1-2, pp. 146–153, (2008).

vi. A. P. Steynberg, M. Dry, (eds.), "Fischer–Tropsch Technology," Studies in Surface Science and Catalysis (Volume 152, ISBN: 978-0-444-51354-0), Elsevier Science and Technology Books, Amsterdam, pp. 1–10. (2004).

vii. W. M. Hexana, N. J. Coville, "Indium as a chemical promoter in Fe–based Fischer–Tropsch synthesis" Applied Catalysis A: General, vol 377, no.1-2, pp. 150–157, (2010).

viii. W. X. Zhang, T. X. Sun, W. Guan, D. Liang, L. Lin, "Enhanced activity of an In–Fe_2O_3/H–ZSM–5 catalyst for NO reduction with methane,". Applied Catalysis B: Environmental, vol. 24, no. 3-4, pp. 169–173, (2000).

ix. G. Zhao, C. Zhang, S. Qin, H. Xianga, Y. Li, "Effect of interaction between potassium and structural promoters on Fischer–Tropsch performance in iron–based catalysts," Journal of Molecular. Catalysis A: Chemical, vol. 286, no. 1-2, pp. 137–142, (2008).

x. J. L. G. Fierro, "Reverse toptactic transformation of a Cu–Zn–Al catalyst during wet Pd–impregnation: Relevance for the performance of methanol synthesis from CO_2/H_2 mixture," Journal of Catalysis, vol. 210, no. 2, pp. 273–284, (2002).